






Original Article


Geochemical characteristics and growth suitability assessment of *Scutellaria baicalensis* Georgi in the Earth's critical zone of North China


LI Xia^{1,2}  <https://orcid.org/0000-0003-1325-1557>; e-mail: lx2003cg@163.com


WEI Xiao-feng³  <https://orcid.org/0000-0003-1250-5893>; email: yanchixiaowei@163.com

WU Jin^{4*}  <https://orcid.org/0000-0001-5653-8561>;  e-mail: WuJin@bjut.edu.cn

YIN Zhi-qiang²  <https://orcid.org/0000-0003-2706-4429>; e-mail: yinzhiqiang@mail.cgs.gov.cn

WAN Li-qin²  <https://orcid.org/0000-0002-3918-456X>; e-mail: 313273589@qq.com

SUN Hou-yun⁵  <https://orcid.org/0000-0002-3511-3879>; e-mail: shyun@cugb.edu.cn

AN Yong-long²  <https://orcid.org/0000-0002-0557-6709>; e-mail: aylzlj@163.com

*Corresponding author

¹ College of Water Sciences, Beijing Normal University, Beijing 100875, China

² China Institute of Geo-Environment Monitoring, Beijing 100081, China

³ Beijing Institute of Geology for Mineral Resources, Beijing 100012, China

⁴ Faculty of Architecture, Civil and Transportation Engineering, Beijing University of Technology, Beijing 100124, China

⁵ School of Water Resources & Environment, China University of Geosciences, Beijing 100083, China

Citation: Li X, Wei XF, Wu J, et al. (2022) Geochemical characteristics and growth suitability assessment of *Scutellaria baicalensis* Georgi in the Earth's critical zone of North China. Journal of Mountain Science 19(5). <https://doi.org/10.1007/s11629-021-7015-9>

© Science Press, Institute of Mountain Hazards and Environment, CAS and Springer-Verlag GmbH Germany, part of Springer Nature 2022

Abstract: Geochemical differentiation of soils has a series of consequences on plant and places pressure on the ecological environment. The quantitative evaluation of element migration in the Earth's critical zone is a challenging task. In this study, two demonstration study areas of *Scutellaria baicalensis* Georgi were selected, and multiple chemical weathering indexes, chemical loss fraction, mass migration coefficients and biological enrichment coefficient method were used to assess the ecological and geochemical suitability. The results show that for the element of Fe, Zn, Se, Cu, Co, Ni, Mo and Ge, the degree of weathering and soil maturation, were greater in the rhyolitic tuff area than in the

Plagioclase gneiss area. In both research sites, the heavy metal level of samples in *Scutellaria baicalensis* Georgi did not exceed the standard limits. The plagioclase gneiss region's surface soil environment was more alkaline, and the content of soil organic matter was lower, resulting in a higher bioenrichment intensity of Ge, Co, Cu, and Se elements in *Scutellaria baicalensis* Georgi than in the rhyolite-tuff area. The elements of Cd, Nb, Mo, Pb and As are considerably enriched in the soil of the plagioclase gneiss area but lost by leaching in the soil of the rhyolite tuff area, which is connected to the interplay of elemental abundance and human impact in the parent materials. This study provides a good example of how to assess growth suitability of Chinese medicinal materials in the Earth's critical zone.

Received: 19-Jul-2021

1st Revision: 25-Jan-2022

2nd Revision: 15-Feb-2022

Accepted: 02-Mar-2022

Keywords: Earth's critical zone; Biogeochemistry characteristics; Weathering mechanism; Element migration; Chinese medicinal materials; Chengde

1 Introduction

Scutellaria baicalensis Georgi, a perennial herb, is one of the most commonly used Chinese medicinal herbs. It has the functions of clearing heat and dampness, purging fire, clearing the heart, cooling blood and promoting blood circulation and plays an important role in the prevention and control of the new coronavirus epidemic (Lam et al. 2010; Wang et al. 2018; Zhi et al. 2020). At present, researches on *Scutellaria baicalensis* Georgi have mostly focused on the contents of active ingredients, fingerprints, pharmacology, etc. (Amber and Viqar 2015; Bokhari and Syed 2015; Zhao et al. 2016b; Cheng et al. 2018; Braude and Bassily 2019; Jin et al. 2019). Studies on the environmental conditions of plants have mostly focused on the climate, geomorphology, rhizosphere soil, etc. but few studies have examined the growth of *Scutellaria baicalensis* Georgi with regards to element migration and aggregation in Earth's critical zone systems (Kong 2008; Pen 2011; Zhao et al. 2018).

The Earth's critical zone is a heterogeneous near-surface environment with active ecological and geochemical processes. It is the area of intersection of material migration and energy exchange in the Earth's surface system, presenting an obvious vertical conduction inheritance law (Lin 2010; Alaimo et al. 2018; Sun et al. 2020). The concept of an "ecosystem" in ecology is significantly consistent with the "key zone" in Earth science (Richter et al. 2015). As an important source of soil parent material, rocks and sediments directly determine the diversity and differences in the physical and chemical properties, elemental abundances and spatial distributions of soils (Vigil et al. 1993; Zhang et al. 2005; Anderson 2015; Li et al. 2019), which restrict the growth and quality of plants. The soil layer, as the core element connecting the Earth's key zonal elements and processes, is an important node controlling the migration and transformation of geochemical elements (Peng et al. 2014; Zhang et al. 2015; An et al. 2016; Lv et al. 2017; An et al. 2018; Luo et al. 2019). The Earth's critical zone is a comprehensive study of the element migration and accumulation of the rock-weathering crust-soil-plant systems (Holl et al. 2007;

Guo et al. 2013; He et al. 2016; Laila et al. 2019). It is an important indicator for the ecological geochemical characteristics, yield and improvement of quality for the *Scutellaria baicalensis* Georgi. Therefore, it is necessary to study the regional chemical characteristics of *Scutellaria baicalensis* Georgi to improve its cultivation efficiency.

Wild quality *Scutellaria baicalensis* Georgi is mainly distributed in the northern mountainous area of the Greater Hinggan Mountains in southwestern China (Guo et al. 2014; Zhao et al. 2016a; Xu et al. 2020). In recent years, wild *Scutellaria baicalensis* Georgi has faced changes due to its ecologically suitable environment and resource shrinkage. The yield of *Scutellaria baicalensis* Georgi in 2020 was 6.67×10^4 hm² (Sun et al. 2020). The soil of the Earth's critical zone in the North China mountainous area is mainly formed by the nearby weathering of bedrock, which has the characteristics of deposited parent material and can best reflect the background characteristics of natural resources (Chadwick et al. 1990; Brantley et al. 2007; Hewawasam et al. 2013; Zhang et al. 2019). This region represents a typical critical earth zone for studying the appropriate growth characteristics of authentic Chinese medicinal materials.

Therefore, the main objectives of this research are (1) to establish a set of different key geochemical elemental migration, accumulation and distribution characteristics, (2) to explore the key rock weathering soil supergene geological processes and the overall dynamic plant growth and ecological geochemical behaviors, and (3) to identify the suitable relationships between the physical and chemical characteristics of the Earth and the Chinese *Scutellaria baicalensis* Georgi to assess the ecological and geochemical suitability of this medicinal plant and to provide a scientific basis for oriented cultivation planning.

2 Materials and Methods

2.1 Overview of research area

The research areas are located in Xiayingzi Village, Jingoutun Town and in Wudaoling Village, Zhangbaiwan Town in Luanping County, Chengde City, Hebei Province, China (Fig. 1). This is the main producing area of the *Scutellaria baicalensis* Georgi

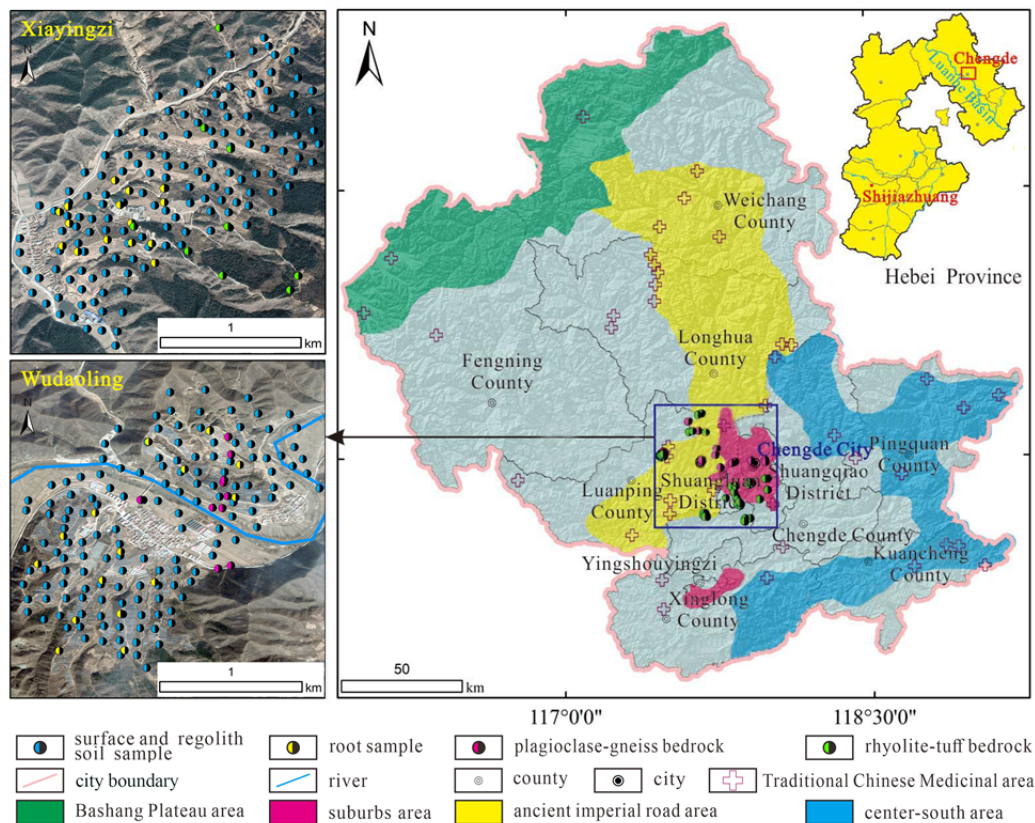


Fig. 1 Geographic and sampling locations in two study areas in Chengde City, Hebei Province, China.

in the northern part of the Yanshan Mountain range that is connected to the Greater Khingan Mountains to the southwest. This area has a semiarid and semihumid continental monsoon climate, with an average annual precipitation of 351.1 mm, most of which occurs from June to August. *Scutellaria baicalensis* Georgi is mainly distributed in northeastern Inner Mongolia, parts of Hebei and southwestern Liaoning Province in China. Chengde is a high quality producing area of *Scutellaria baicalensis* Georgi (Zhao et al. 2016a). The Zhangjiakou Formation (J_3z) andesite, crystal tuff, fused tuff, rhyolitic tuff lava and rhyolitic brecciated tuff are mainly exposed in the Xiayingzi demonstration zone. The main rock minerals are approximately 45%-50% plagioclase, approximately 25% potash feldspar and approximately 15%-20% quartz. The rocks are mainly composed of volcanic breccia and tuff. The volcanic breccia is rhyolite, rhyolite fused tuff, rhyolite fused tuff, containing magnetite, apatite, sericite, kaolinite and other minerals. The Neoproterozoic Zhongyingzi (Ar_3Zgn) gray-white plagioclase gneiss and plagioclase leucocleptite are mainly exposed in the Wudaoling demonstration zone. The rocks are mainly composed

of plagioclase, potassium feldspar, quartz, biotite and hornblende. The original rock is fine-grained granodiorite and other magmatic rocks, such as approximately 65%-70% of plagioclase, approximately 5%-10% potassium feldspar, approximately 5% quartz, and approximately 1%-5% biotite. The soil types in Xiayingzi are shrub cinnamon soil and coarse bone soil. Wudaoling lies on both sides of the main stream of the Luanhe River, with the main soil type being cinnamon soil. However, some moist soil is distributed in the floodplain. The soil texture is mainly sandy and sandy loamy soil, with a strong nutrient holding capacity, high water transport and effectiveness.

2.2 Sample collection and testing

The samples collected in this study are mainly root samples of the *Scutellaria baicalensis* Georgi, surface soil samples, regolith soils and fresh bedrock samples. 15 root samples, 163 surface soil samples, 163 regolith soil samples, and 9 fresh bedrock samples containing rhyolite and tuff volcanic rocks were collected in Xiayingzi. 15 root samples, 162 surface soil samples, 162 regolith soil samples and 6

fresh bedrock samples containing plagioclase gneiss-granulite were collected in Wudaoling.

The N, P, K₂O, CaO, MgO, S, TFe₂O₃, B, Mn, Cu, Zn, Mo, SiO₂, Na₂O, Ni, Se, Ge, Al₂O₃, Co, Cd, Cr, Pb, As, Hg, and rare earth element (La, Ce, Pr, Nd, Sm, Eu, Gd, Tb, Dy, Ho, Er, Tm, Yb, Lu and Y) concentrations of the surface soils, regoliths, and bedrock samples were tested. The pH and organic matter (SOM) indices were also measured in the soil and regolith samples. Fe, B, Cr, Co, Ni, Cu, Zn, As, Pb, Cd, Mo, Se, Ge and rare earth elements were tested in medicinal plant samples. The contents of Se, As and Hg in bedrock and soil samples were tested by a hydride generation atomic fluorometer. The contents of SiO₂, Al₂O₃, Fe₂O₃, MgO, CaO, Na₂O, K₂O, Mn, Ti, P and S were tested by wavelength dispersive X-ray fluorescence spectrometry (ARL Advant XP+/2413). The contents of the other elements were tested by ICP-OES (PE, USA). The elemental contents of the medicinal plant samples were tested by a high-resolution plasma mass spectrometer (X series 2/SNO1831C). The sample testing and analysis were controlled by adding 10% blank samples and parallel samples according to standard requirements. The accuracy and precision of the analytical methods were controlled by national first-level standard material (GBW series). The standard recovery of each index was within the allowable range of national standard reference substances. Detailed analysis of the sample digestion and processing protocols are in the [Appendix 1](#).

2.3 Analysis methods

Based on the sample analysis and test, SPSS was used to conduct descriptive statistics on the test indicators, the geochemical grades of topsoil elements were determined by referring to the Land Quality Geochemical Evaluation Standard (DZ/T 0295-2016), and the distribution characteristics of elements in the bedrock, regolith, soil layer and medicinal plants were compared. The silicon-aluminium-ferrum ratio (SAF), chemical index of alteration (CIA), mineralogical index of alteration (MIA), and weathering leaching (BA) were used to evaluate the influence of weathering degree on the release, migration and accumulation of elements in the process of soil formation. Using the chemical depletion fraction (CDF) in the process of quantitative evaluation of rock and soil release, migration and accumulation and

using the bioconcentration factor (BCF) to evaluate the element migration and accumulation characteristics of the soil-medicinal plant layer, the suitable ecological geochemistry of the *Scutellaria baicalensis* Georgi growing conditions was determined. Residual factor (RF) is a commonly used indicator of clay weathering development, reflecting the relative enrichment or residual degree of stable elements Fe and Al. The higher the RF value, the stronger the leaching effect of Ca, Mg and Na elements, and the more residual elements of Al and Fe, which is reflecting the higher the degree of weathering and the stronger the soil-forming.

2.3.1 Chemical depletion fraction

The weathering index mainly represents the dispersion and enrichment characteristics of major elements in the process of mineral weathering, and for trace and rare earth elements, the migration and accumulation characteristics during the weathering process, the CDF can be used according to the mass conservation principle to represent the leaching and enrichment of elements during bedrock weathering (Eduardo et al. 2014, Oeser et al. 2018). In the process of chemical weathering, CDF can be a good measure of the profit and loss of the elements in the regolith. The calculation method is as follows:

$$CDF = 1 - \frac{[X_i]_{\text{parent}}}{[X_i]_{\text{weathered}}} \quad (1)$$

where X_i represents the measured value of corresponding elements in the soil and bedrock; $[X_i]_{\text{parent}}$ represents the content of corresponding elements of fresh bedrock; $[X_i]_{\text{weathered}}$ represents the content value of corresponding elements in regolith or soil.

2.3.2 Bios index methods

The silicon-aluminum-ferrum ratio (SAF), chemical index of alteration (CIA), and MIA reveal crustal elements and are key trace nutrient element indicators to evaluate the influence of the weathering process on the release, migration and accumulation of rocky elements. The calculation methods are shown in [Table 1](#).

IOL indices were calculated using the mass fraction of oxides. Other weathering indices were calculated using the molecular molar number of oxides. CaO* is the molar content of silicate minerals, excluding the content of CaO in carbonate and phosphate minerals. Since CaO and Na₂O in silicate usually exist in a molar ratio of 1:1, when the number of CaO is greater than Na₂O, the molecular mole of

Table 1 Equation of calculation formula of biological index

| Indicators | Equation formula | Reference |
|--|---|--------------------------------|
| Silicon-aluminium-ferrum ratio (SAF) | $SiO_2 / (Al_2O_3 + Fe_2O_3)$ | Qiu et al. 2014 |
| Residual factor (RF) | $[(Al_2O_3 + Fe_2O_3) / (CaO^* + Na_2O + MgO)]$ | Qiu et al. 2014 |
| Index of laterization (IOL) | $[(Al_2O_3 + Fe_2O_3) / (Al_2O_3 + Fe_2O_3 + SiO_2)] \times 100$ | Babechuk et al. 2014 |
| Chemical index of alteration (CIA) | $[Al_2O_3 / (Al_2O_3 + CaO^* + Na_2O + K_2O)] \times 100$ | Nesbitt and Young (1982, 1984) |
| Mafic index of alteration oxidation (MIAo) | $[Al_2O_3 / (Al_2O_3 + Fe_2O_3 + MgO + CaO^* + Na_2O + K_2O)] \times 100$ | Babechuk et al. 2014 |
| Mafic index of alteration reduction (MIAr) | $[(Al_2O_3 + Fe_2O_3) / (Al_2O_3 + Fe_2O_3 + MgO + CaO^* + Na_2O + K_2O)] \times 100$ | Babechuk et al. 2014 |
| Index of chemical variation (ICV) | $[(Fe_2O_3 + MgO + CaO^* + Na_2O + K_2O + MnO + TiO_2) / Al_2O_3]$ | Cox et al. 1995 |

Notes: IOL indices were calculated using the mass fraction of oxides. Other weathering indices were calculated using the molecular molar number of oxides. CaO* is the molar content of silicate minerals, excluding the content of CaO in carbonate and phosphate minerals. Since CaO and Na₂O in silicate usually exist in a molar ratio of 1:1, when the number of CaO is greater than Na₂O, the molecular mole of CaO* is equal to the molecular mole of Na₂O, while when the number is less than Na₂O, mCaO*=mCaO.

CaO* is equal to the molecular mole of Na₂O, while when the number is less than Na₂O, mCaO*=mCaO.

2.3.3 Bioconcentration factor of elements

BCF was used to characterize the distribution characteristics of elements in the soil-*Scutellaria baicalensis* Georgi system (Yang et al. 2017, Midhat et al. 2019), whose calculation method is:

$$BCF = \frac{[X_i]_{plant}}{[X_i]_{soil}} \quad (2)$$

where [X_i]_{plant} and [X_i]_{soil} represent the content of element I in medicinal plant samples and in soil samples, respectively. According to the bioconcentration coefficient, the uptake intensity of the soil elements by medicinal plants can be divided into four grades: strong uptake at BCF>1.0, moderate uptake at 0.1<BCF≤1.0, weak uptake at 0.01<BCF≤0.1, and very weak uptake at BCF<0.01.

3 Results and Discussion

3.1 Soil elemental content characteristics of *Scutellaria baicalensis* Georgi

The elemental contents of the bedrock-regolith-topsoil in two typical demonstration zones of *Scutellaria baicalensis* Georgi in Xiayingzi and Wudaoling (Table 2) were calculated from regional statistics, and then the topsoil elemental geochemical grades were determined by referring to the

Specification of Land Quality Geochemical Assessment (DZ/T 0295-2016). The proportion of each elemental geochemical grade is shown in Fig. 2.

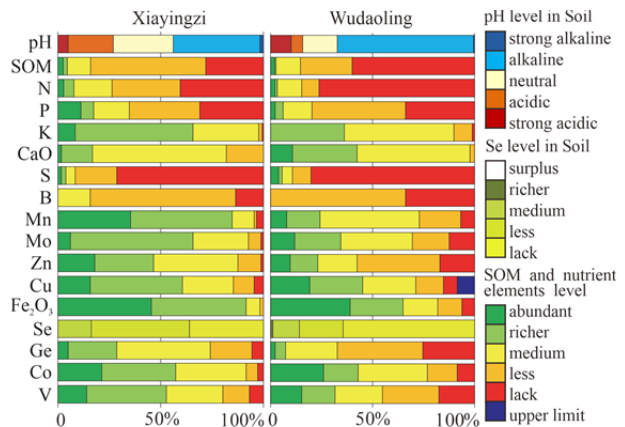


Fig. 2 pH, SOM and nutrient elemental geochemical land quality grades of surface soil in Xiayingzi and Wudaoling, in Chengde City, Hebei Province, China.

Different lithology of bedrock may result in differences in topsoil types and element content. Significant differences of most element content in the soil were found between the typical areas (P<0.1). Significant differences were also found in regolith soil (such as Cu, Zn, Mo, Mn, Pb, Cr) between the typical areas (P<0.1). Significant differences were also found in bedrock (such as Zn, Mo, Mn, Pb, Al, K) between the typical areas (P<0.1).

The soil in the rhyolite tuff area of Xiayingzi was mainly neutral-alkaline, with a pH range of 5.00~8.50 and an average value of 7.17; therefore, 42.13% of the

Table 2 Statistics of geochemical elemental contents of the bedrock-regolith-soil samples.

| Element | Soil | | | | | |
|------------------------------------|------------------|----------------------|-------|------------------|----------------------|-------|
| | Xiayingzi | | | Wudaoling | | |
| | Min-Max | Mean | CV | Min-Max | Mean | CV |
| N (mg/kg) | 346.000-2917.000 | 852.550** | 0.430 | 98.000-2745.000 | 688.667** | 0.587 |
| P (mg/kg) | 156.100-5349.000 | 790.780** | 1.150 | 137.900-1619.000 | 492.745** | 0.429 |
| S (mg/kg) | 76.230-460.300 | 158.220 | 0.310 | 61.680-413.400 | 147.536 | 0.435 |
| B (mg/kg) | 6.010-49.810 | 37.930** | 0.250 | 4.209-45.600 | 31.640** | 0.322 |
| Cu (mg/kg) | 9.320-41.250 | 25.010** | 0.180 | 10.940-83.840 | 28.600** | 0.499 |
| Zn (mg/kg) | 54.670-256.100 | 77.590** | 0.320 | 27.440-209.100 | 62.860** | 0.318 |
| Mo (mg/kg) | 0.392-1.290 | 0.691 | 0.163 | 0.268-2.936 | 0.688 | 0.539 |
| Se (µg/kg) | 0.078-0.290 | 0.141** | 0.275 | 0.045-0.417 | 0.125** | 0.434 |
| Ge (µg/kg) | 1.017-1.859 | 1.352** | 0.079 | 0.987-2.056 | 1.268** | 0.093 |
| Mn (mg/kg) | 393.700-2075.000 | 718.330** | 0.270 | 313.600-1191.000 | 561.376** | 0.244 |
| V (mg/kg) | 27.830-161.200 | 85.570* | 0.230 | 29.610-206.600 | 78.865* | 0.320 |
| Co (µg/kg) | 3.950-38.563 | 14.477 | 0.334 | 5.264-38.420 | 13.690 | 0.392 |
| Cd (µg/kg) | 0.055-0.633 | 0.132** | 0.401 | 0.035-0.338 | 0.113** | 0.422 |
| Cr (mg/kg) | 20.735-228.360 | 69.025 | 0.297 | 20.526-411.620 | 75.012 | 0.730 |
| Pb (µg/kg) | 15.040-42.209 | 24.591 | 0.155 | 8.937-319.500 | 22.469 | 1.120 |
| Ni (mg/kg) | 9.841-116.900 | 34.965** | 0.331 | 4.476-122.200 | 30.878** | 0.480 |
| As (mg/kg) | 3.176-21.411 | 11.319** | 0.253 | 1.808-15.894 | 8.955** | 0.335 |
| Hg (µg/kg) | 0.010-0.200 | 0.025 | 0.720 | 0.007-1.774 | 0.043 | 3.457 |
| SOM (mg/kg) | 0.212-6.625 | 1.491** | 0.597 | 0.178-5.847 | 1.158** | 0.722 |
| TC (mg/kg) | 0.074-3.263 | 1.309** | 0.576 | 0.447-2.110 | 1.347** | 0.399 |
| SiO ₂ (%) | 52.260-75.680 | 64.720** | 0.070 | 53.404-67.049 | 60.345** | 0.066 |
| Al ₂ O ₃ (%) | 11.110-18.680 | 14.060** | 0.110 | 11.721-15.059 | 13.804** | 0.085 |
| K ₂ O (%) | 0.720-5.490 | 2.540** | 0.200 | 0.832-2.636 | 2.244** | 0.142 |
| Na ₂ O (%) | 1.360-3.310 | 2.110** | 0.220 | 1.551-3.427 | 2.497** | 0.233 |
| CaO (%) | 0.580-6.100 | 1.950** | 0.590 | 0.993-8.729 | 2.993** | 0.562 |
| MgO (%) | 0.720-2.650 | 1.570** | 0.280 | 1.623-127.100 | 13.538** | 2.782 |
| Fe ₂ O ₃ (%) | 3.870-9.840 | 5.530 | 0.200 | 2.441-14.810 | 5.380 | 0.324 |
| pH | 5.000-8.500 | 7.171** | 0.133 | 4.990-8.730 | 7.886** | 0.095 |
| LREE (mg/kg) | 159.017-436.394 | 206.985** | 0.278 | 114.174-198.761 | 150.016** | 0.172 |
| HREE (mg/kg) | 38.928-59.289 | 49.085** | 0.118 | 23.925-50.029 | 38.220** | 0.185 |
| REE (mg/kg) | 197.945-495.683 | 256.070** | 0.241 | 146.696-248.790 | 188.235** | 0.167 |
| LR/HR | 3.524-7.360 | 4.186** | 0.184 | 3.361-5.695 | 3.980** | 0.166 |
| Element | Regolith | | | | | |
| | Xiayingzi | | | Wudaoling | | |
| | Min-Max | Mean | CV | Min-Max | Mean | CV |
| N (mg/kg) | 79.000-2811.000 | 366.330 | 1.190 | 131.000-955.000 | 303.333 | 0.838 |
| P (mg/kg) | 107.700-5444.000 | 841.530 | 1.350 | 642.300-2324.500 | 1190.358 | 0.410 |
| S (mg/kg) | 32.200-592.800 | 115.010 | 0.900 | 6.918-161.100 | 72.591 | 0.543 |
| B (mg/kg) | 1.860-49.630 | 17.500 | 0.760 | 2.339-29.570 | 9.175 | 0.804 |
| Cu (mg/kg) | 1.760-64.330 | 22.740 ^a | 0.600 | 17.570-59.900 | 45.348 ^a | 0.303 |
| Zn (mg/kg) | 50.100-204.380 | 100.410 ^b | 0.330 | 49.450-125.300 | 83.103 ^a | 0.239 |
| Mo (mg/kg) | 0.045-13.560 | 1.145 ^b | 1.799 | 0.275-1.043 | 0.418 ^a | 0.498 |
| Se (µg/kg) | 0.030-0.218 | 0.083 | 0.554 | 0.047-0.145 | 0.090 | 0.327 |
| Ge (µg/kg) | 0.916-1.765 | 1.279 | 0.171 | 0.741-1.551 | 1.097 | 0.169 |
| Mn (mg/kg) | 40.460-2742.000 | 836.690 | 0.600 | 413.300-1368.000 | 717.992 ^b | 0.371 |
| V (mg/kg) | 7.710-489.800 | 70.510 | 1.080 | 55.740-230.800 | 112.023 | 0.385 |
| Co (µg/kg) | 0.979-36.270 | 10.559 | 0.805 | 8.978-34.050 | 19.711 | 0.332 |
| Cd (µg/kg) | 0.021-1.655 | 0.185 | 1.424 | 0.031-0.125 | 0.082 | 0.369 |
| Cr (mg/kg) | 3.100-369.700 | 45.523 ^b | 1.237 | 12.210-211.200 | 78.618 | 0.742 |
| Pb (µg/kg) | 10.689-85.550 | 23.689 ^a | 0.487 | 7.980-24.203 | 16.533 ^a | 0.280 |
| Ni (mg/kg) | 2.198-52.430 | 19.092 | 0.698 | 11.520-58.890 | 30.625 | 0.480 |
| As (mg/kg) | 0.715-148.800 | 11.485 | 2.507 | 1.873-8.327 | 4.136 | 0.477 |
| Hg (µg/kg) | 0.003-0.104 | 0.018 | 1.207 | 0.005-0.030 | 0.012 | 0.567 |
| SOM (mg/kg) | 0.031-1.500 | 0.305 | 0.957 | 0.077-1.287 | 0.275 | 1.368 |

(-To be continued-)

(-Continued-) **Table 2** Statistics of geochemical elemental contents of the bedrock-regolith-soil samples.

| Element | Regolith | | | | | |
|------------------------------------|-----------------|---------|-------|-----------------|---------|-------|
| | Xiayingzi | | | Wudaoling | | |
| | Min-Max | Mean | CV | Min-Max | Mean | CV |
| TC (mg/kg) | 0.030-3.999 | 0.446 | 1.452 | 0.099-1.298 | 0.374 | 1.172 |
| SiO ₂ (%) | 43.460-77.580 | 64.090 | 0.120 | 54.163-68.237 | 60.327 | 0.070 |
| Al ₂ O ₃ (%) | 9.910-20.310 | 14.870 | 0.130 | 13.539-18.357 | 15.656 | 0.101 |
| K ₂ O (%) | 1.310-7.630 | 3.380 | 0.420 | 1.000-4.000 | 2.612 | 0.322 |
| Na ₂ O (%) | 0.380-6.700 | 2.610 | 0.470 | 2.107-5.112 | 3.592 | 0.274 |
| CaO (%) | 0.280-18.330 | 2.050 | 1.380 | 1.065-6.260 | 3.045 | 0.435 |
| MgO (%) | 0.150-2.710 | 1.330 | 0.470 | 0.983-134.100 | 14.227 | 2.795 |
| Fe ₂ O ₃ (%) | 1.450-10.330 | 5.080 | 0.400 | 3.726-10.353 | 6.633 | 0.261 |
| pH | 5.230-9.350 | 7.117 | 0.122 | 6.440-8.480 | 7.467 | 0.101 |
| LREE (mg/kg) | 95.557-481.326 | 282.578 | 0.372 | 140.530-368.731 | 210.092 | 0.450 |
| HREE (mg/kg) | 12.266-79.066 | 55.032 | 0.293 | 18.736-45.292 | 30.713 | 0.353 |
| REE (mg/kg) | 107.823-538.298 | 337.610 | 0.348 | 164.296-414.023 | 240.804 | 0.420 |
| LR/HR | 3.370-8.448 | 5.238 | 0.279 | 4.005-12.005 | 7.198 | 0.425 |

| Element | Bedrock | | | | | |
|------------------------------------|-----------------|----------------------|-------|------------------|----------------------|-------|
| | Xiayingzi | | | Wudaoling | | |
| | Min-Max | Mean | CV | Min-Max | Mean | CV |
| N (mg/kg) | 48.000-630.000 | 130.670 | 0.750 | 72.000-342.000 | 124.190 | 0.440 |
| P (mg/kg) | 77.840-5479.000 | 1097.770 | 1.380 | 257.700-1517.000 | 813.733 | 0.543 |
| S (mg/kg) | 29.840-1557.000 | 131.110 | 2.060 | 0.721-205.600 | 60.979 | 0.890 |
| B (mg/kg) | 1.390-40.700 | 7.490 | 0.930 | 1.501-13.360 | 4.709 | 0.673 |
| Cu (mg/kg) | 2.690-388.100 | 44.390 | 1.340 | 0.549-156.100 | 47.687 | 0.741 |
| Zn (mg/kg) | 30.700-371.900 | 114.800 ^α | 0.470 | 29.410-155.300 | 87.285 ^α | 0.393 |
| Mo (mg/kg) | 0.090-56.000 | 2.090 ^β | 3.780 | 0.135-1.045 | 0.390 ^α | 0.670 |
| Se (μg/kg) | 0.002-0.208 | 0.048 | 0.820 | 0.017-0.223 | 0.064 | 0.778 |
| Ge (μg/kg) | 0.538-2.190 | 1.271 | 0.269 | 0.768-1.581 | 1.053 | 0.204 |
| Mn (mg/kg) | 20.950-1892.000 | 689.740 ^β | 0.580 | 55.490-2019.000 | 654.940 ^β | 0.782 |
| V (mg/kg) | 4.660-413.700 | 69.110 | 1.220 | 11.440-377.500 | 101.583 | 0.802 |
| Co (μg/kg) | 0.414-62.680 | 11.256 | 1.218 | 2.120-46.970 | 17.755 | 0.708 |
| Cd (μg/kg) | 0.020-0.760 | 0.130 | 1.096 | 0.017-0.324 | 0.092 | 0.804 |
| Cr (mg/kg) | 1.600-133.000 | 33.482 | 1.090 | 3.752-300.600 | 93.927 | 0.920 |
| Pb (μg/kg) | 3.514-134.400 | 22.906 ^α | 0.761 | 5.154-45.860 | 17.494 ^α | 0.621 |
| Ni (mg/kg) | 1.718-63.760 | 16.706 | 1.029 | 2.719-105.500 | 34.344 | 0.788 |
| As (mg/kg) | 0.528-723.400 | 23.536 | 4.594 | 0.412-21.750 | 3.339 | 1.426 |
| Hg (μg/kg) | 0.002-0.113 | 0.022 | 1.419 | 0.002-0.016 | 0.005 | 0.512 |
| SOM(mg/kg) | 0.023-0.787 | 0.102 | 1.121 | 0.047-0.540 | 0.223 | 0.684 |
| TC (mg/kg) | 0.024-0.740 | 0.133 | 0.910 | 0.019-0.420 | 0.081 | 1.088 |
| SiO ₂ (%) | 46.550-85.290 | 66.630 | 0.140 | 0.128-77.288 | 56.998 | 0.361 |
| Al ₂ O ₃ (%) | 7.720-19.620 | 14.610 ^β | 0.130 | 13.315-18.740 | 14.856 ^β | 0.091 |
| K ₂ O (%) | 0.610-9.900 | 3.980 ^β | 0.530 | 0.585-5.652 | 3.003 ^β | 0.501 |
| Na ₂ O (%) | 0.410-5.980 | 3.160 | 0.390 | 1.326-4.151 | 3.123 ^β | 0.251 |
| CaO (%) | 0.050-9.080 | 2.120 | 1.000 | 0.434-7.992 | 3.034 | 0.776 |
| MgO (%) | 0.110-6.180 | 1.350 | 0.900 | 0.293-131.000 | 10.846 | 2.826 |
| Fe ₂ O ₃ (%) | 0.710-16.250 | 5.130 | 0.640 | 1.402-14.944 | 6.091 | 0.556 |
| pH | 5.970-9.670 | 7.531 | 0.112 | 0.118-9.610 | 6.943 | 0.369 |
| LREE (mg/kg) | 8.870-468.770 | 248.233 | 0.502 | 102.243-304.824 | 154.965 | 0.454 |
| HREE (mg/kg) | 2.476-83.440 | 46.719 | 0.453 | 12.068-31.199 | 20.569 | 0.288 |
| REE (mg/kg) | 11.346-525.111 | 294.952 | 0.483 | 121.043-321.032 | 175.535 | 0.396 |
| LR/HR | 3.017-8.320 | 5.340 | 0.266 | 3.975-18.807 | 8.210 | 0.579 |

1) Min represents the minimum value; Max represents the maximum value; Mean represents the average value, ** represents the ANOVA confidence interval of soil is less than 0.05, *indicates the ANOVA confidence interval of the soil is less than 0.1, indicates the ANOVA confidence interval of regolith is less than 0.05, b indicates the ANOVA confidence interval of regolith is less than 0.1, α indicates the ANOVA confidence interval of the bedrock is less than 0.05, β indicates the ANOVA confidence interval of bedrock is less than 0.1; CV represents the coefficient of variation; and pH and LREE/HREE are dimensionless.

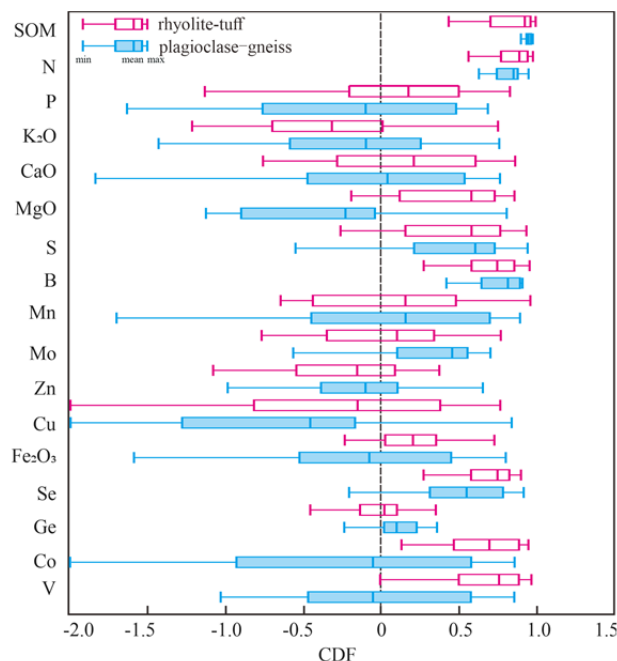
soil samples were alkaline, 29.21% of them were neutral, and 21.91% of them were acidic. The geochemical grades were mainly deficient-relatively deficient, among which 65.17% of the samples were deficient-relatively deficient, whereas 17.42% of the samples were rich-abundant. The geochemical grade of the land quality was medium, accounting for 65.17%, whereas rich-relatively rich level samples only accounted for 16.85%. The content of Al_2O_3 in the soil ranged from 11.11% to 18.68%, with an average of 14.06%. The content of soil organic matter (SOM) ranged from 0.21% to 6.63%, with an average content of 1.49%, mainly as deficient-relatively deficient; in contrast, the proportion of rich-abundant samples was 4.67%. Except for MgO, CaO, Na_2O , Hg, Cu and Cr, the contents of elements in the Wudaoling area were higher than those in the Xiayingzi area, and the contents of other elements in the Xiayingzi area were all higher than those in the Wudaoling area, among which the contents of P and rare earth elements were significantly different and the contents of TFe_2O_3 , Al_2O_3 , Co and Mo were relatively similar.

3.2 Soil-bedrock elemental chemical depletion fraction (CDF)

The CDFs are used to characterize the elemental enrichment or leaching loss during the weathering and soil-forming processes of the rhyolite tuff bedrock in Xiayingzi and in plagioclase gneiss in Wudaoling. The CDF box plots of the two study areas are shown in Fig. 3. The CDF values of the elements in the bedrock-soil profile in the Xiayingzi area were ranked as $TN > SOM > B > Se > Ni > Cr > S > V > MgO > Co > Sr > Ti > TFe_2O_3 > Ge > O$ and were relatively enriched in the process of rock weathering. According to the results, $Na_2O < Cu < As < Nb < Mo < Cd < K_2O < Zn < P < Mn < SiO_2 < Al_2O_3 < Pb < CaO < O$, leaching loss was observed. In the process of rock weathering, the migration chemical behavior of Ge, TFe_2O_3 , Ti, Sr, Co, CaO, Pb, Al_2O_3 and SiO_2 was relatively similar, and the contents in the soil, regolith, and bedrock samples were relatively stable. The contents of TFe_2O_3 , Ti, Sr and Co in soil were characterized by relatively fresh bedrock weak enrichment, and the contents of CaO, Pb, Al_2O_3 and SiO_2 were related to bedrock erosion but had a low degree of leaching loss. The statistical coefficient variation (CV) of the CDF values of CaO, Ge, Pb, Co, TFe_2O_3 and Ti in different sections was relatively large, and the fluctuation differentiation was particularly

obvious. The relative enrichment degree of TN and SOM is the highest, which is also related to the accumulation of organic matter in the growth process of microorganisms and lower plants, nitrogen fixation of higher plants and formation of humus layer in deciduous leaves (Zhu et al. 2014, 2015). B, Se, Ni, Cr, S, V and MgO are all relatively enriched, and the degree of enrichment is relatively high. In the weathering process, Na_2O , K_2O and rare earth elements (REEs, LREs and HREs) all showed leaching loss, and the leaching intensity increased successively, with strong activity.

The CDF values in the bedrock-soil profile of the plagioclase gneiss in Wudaoling were $SOM > TN > B > As > Se > S > LRE > Mo > Nb > Ge > REE > Cd > Ti > Pb > LRE > O$, which represented relative enrichment in the process of rock weathering. $Cu < Sr < Na_2O < MgO < P < Co < CaO < K_2O < Cr < TFe_2O_3 < Zn < V < Al_2O_3 < SiO_2 < Mn < Ni < O$, which manifested as leaching loss in the process of rock weathering. The concentrations of As, Cd and Pb elements in the soil of the plagioclase gneiss area are higher than those in the Xiayingzi area. The Wudaoling *Scutellaria baicalensis* Georgi area is a demonstration base for the photovoltaic industry and plantations, which brings the human influence of heavy metal accumulation in the soil stronger than



Note: Boxes represent 90% confidence intervals
Fig. 3 Statistical box plot of the chemical depletion fraction in the rhyolite-tuff and plagioclase-gneiss geological formations.

that in the Xiayingzi area. The chemical depletion behavior of Co, Cr, TFe_2O_3 and V in the soil was contrary to that of the Xiayingzi area, which showed relatively fresh bedrock leaching loss.

The metamorphic protolith of anorthosite gneisses in the Wudaoling area is mafic granite, mainly composed of minerals such as plagioclase, potash feldspar, biotite, and hornblende. The composition of plagioclase is relatively high, the metamorphism degree of the rock is relatively high, and it is easily weathered. During the rock weathering process, the iron group elements show leaching loss. The tuff of the Zhangjiakou Formation in the Xiayingzi area is the surrounding rock of the vanadium-titanium magnetite deposit, and the content abundance of iron group elements is higher than that in the Wudaoling area. In the rock weathering process, refractory magnetite, apatite, ilmenite and hematite are relatively enriched, while Co, Cr, Ti, TFe_2O_3 and V are relatively enriched. The leached strength of Al_2O_3 and SiO_2 is higher than that of tuff during the weathering process of plagioclase gneiss, which is strongly active and related to the weathering of feldspar minerals.

In the rock weathering process, the enrichment of Ge, B, S, Se and Ti in the construction area of the plagioclase gneiss was higher than that in the construction area of fluorite-tuff, and the difference in the CDF value of the Ge element chemical loss fraction was the largest. The leaching loss of CaO, Al_2O_3 and Cu in the rhyolite tuff area is stronger than that in the plagioclase gneiss area, and the leaching strength of P, SiO_2 , Na_2O , K_2O , Zn and Mn is weaker than that in the plagioclase gneiss area. TFe_2O_3 , Ni, V, Cr, Co, MgO and Sr are relatively enriched in the weathering process of rhyolite-tuff rock, and leaching loss is shown in the weathering process of plagioclase gneiss. Rare earth elements (REEs, LREs and HREs), Cd, Nb, Mo, Pb and As are relatively enriched in the soil of the plagioclase gneiss area and are substance lost by leaching in the soil of the rhyolite tuff area, which is related to the interaction of elemental abundance and human influence in the parent materials.

3.3 Degree of rock weathering on element migration

The weathering degree of the soil is usually characterized by the chemical weathering index, and

the ratio of the main oxide components of rock and soil is used to indicate weathering strength (Moses et al. 2014; Fu et al. 2019; Wen et al. 2019). According to Fig. 4a, the types of rhyolite tuff and plagioclase gneiss in the study area are relatively similar. The rhyolite tuff is mainly composed of aluminum-rich acid volcanic rocks, some of which are medium-alkaline volcanic rocks and basic volcanic rocks.

The CV values of the SAF in bedrock was 0.337, which was relatively greater than that in the topsoil and regolith because of the uneven distribution of breccia in rhyolitic breccia tuff, andesite and ignimbrite and because there were relatively large differences in chemical composition. The SAF values in the plagioclase gneiss geological formation also appeared to be ranked as bedrock>soil>regolith, with a relationship to the large fluctuation in the chemical composition of the weathering crust. The average SAF values of bedrock, regolith and soil were 6.10, 5.30 and 5.90, respectively, which were relatively lower than the values measured in the rhyolite tuff area. The RF values of the bedrock, regolith and soil in the rhyolite tuff area were relatively stable, with average values of 2.05, 2.05 and 1.97, respectively. The RF values of plagioclase gneiss in bedrock, regolith and soil were 1.37, 1.34 and 1.19, respectively, which were related to the relatively enriched CaO, Na_2O and MgO in the weathering process of plagioclase gneiss and the leaching losses of Al_2O_3 and Fe_2O_3 .

The weathering eluviation coefficient was used to reflect the leaching status of Ca, Mg, Na and K. The smaller the weathering leaching (BA) value was, the more obvious the leaching effect of active components was and the stronger the chemical weathering effect was (Qiu et al. 2014). The BA values of the soil ranged from 0.63 to 1.33 in the rhyolite tuff area, from 0.65 to 4.18 in the regolith layer, and from 0.59 to 2.87 in the bedrock layer. The BA values of the soil ranged from 0.78 to 2.16 in the plagioclase gneiss area, from 0.64 to 1.86 in the regolith layer, and from 0.69 to 2.21 in the bedrock layer. As seen from the box plot of the weathering index in Fig. 5, the BA values of samples in each layer of the plagioclase gneiss area were higher than those in the rhyolite tuff area. During the weathering process, Na, Ca and Mg had strong activity, showing the functions of migration and leaching.

The weathering leaching coefficient can only comprehensively reflect the overall leaching characteristics of strongly active elements of alkali

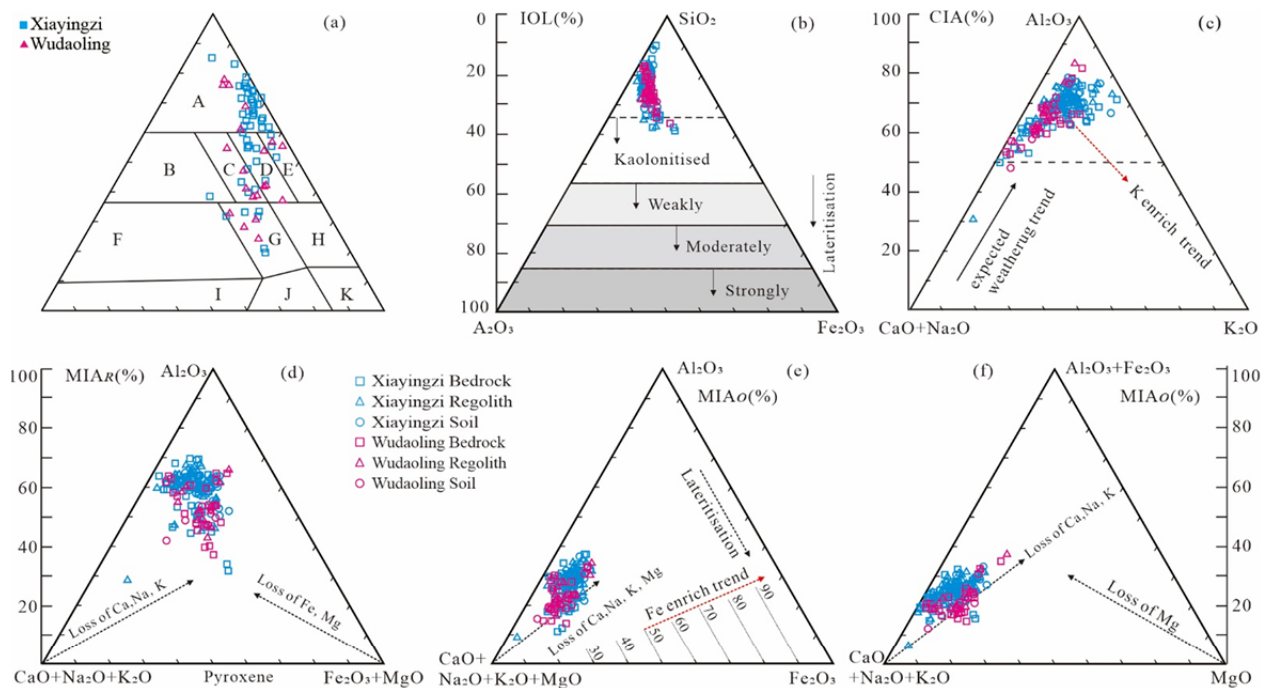


Fig. 4 Discrimination of the protolith and the chemical index of alteration (CIA), index of lateralization (IOL), mineralogical index of alteration (MIA), and original index of the bedrock-regolith-soil samples. (a) Protolith type discrimination chart; (b) $\text{SiO}_2\text{-Al}_2\text{O}_3\text{-Fe}_2\text{O}_3$ (SAF) lateralization index IOL; (c) $\text{Al}_2\text{O}_3\text{-CaO+Na}_2\text{O-K}_2\text{O}$ (A-CN-K) chemical index of alteration (CIA); (d) $\text{Al}_2\text{O}_3\text{-CaO+Na}_2\text{O+K}_2\text{O-Fe}_2\text{O}_3\text{+MgO}$ (A-CN-K-FM) reduction mafic alteration index MIA_R ; (e) $\text{Al}_2\text{O}_3\text{-MgO+CaO+Na}_2\text{O+K}_2\text{O-Fe}_2\text{O}_3$ (A-L-F) magnesium oxide alteration index MIA_o ; (f) $\text{Al}_2\text{O}_3\text{+Fe}_2\text{O}_3\text{-CaO+Na}_2\text{O+K}_2\text{O-MgO}$ (AF-CN-K-M) MgO alteration index.

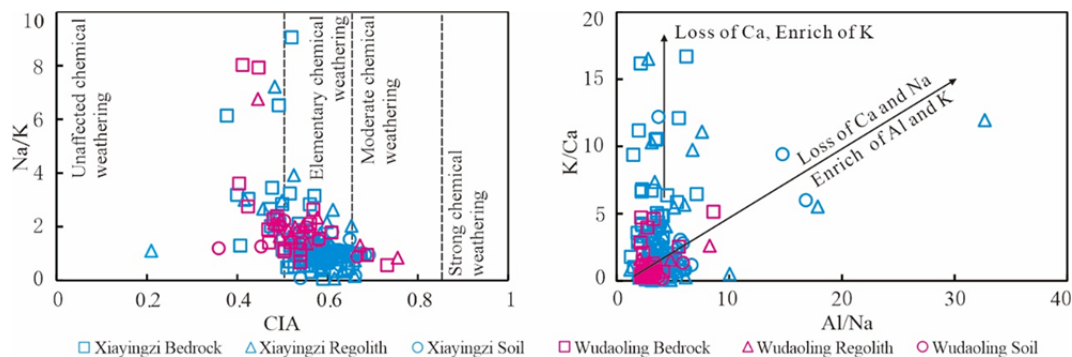


Fig. 5 Relationships of the chemical index of alteration (CIA) with Na/K and K/Ca with Al/Na.

metals and alkaline earth metals. On this basis, the chemical index of alteration (CIA) and mafic index of alteration (MIA) were adopted to reveal the leaching enrichment characteristics of Ca, Mg, Na and K during the weathering process. The CIA was used to reveal the degree of alteration of feldspar into clay minerals and to link rock weathering to climatic conditions (Nesbitt and Young 1982). The higher the CIA value is, the stronger the weathering effect is (Nesbitt and Young 1984). A CIA value between 50 and 65 indicates a low degree of chemical weathering, a CIA value between 65 and 85 indicates a moderate degree of chemical weathering, and a CIA value

between 85 and 100 indicates a strong degree of chemical weathering (Wu et al. 2016).

The results show that the chemical weathering process was at an early stage of decalcification and desodium, at a middle stage of dipotassium and at a late stage of desilication. According to Fig. 5, samples from each layer in the key rhyolite tuff zone were mainly at a stage of primary chemical weathering. The Ca and Na elements were mostly lost due to weathering, and the K element was relatively enriched. The ternary diagram of continental weathering trends (Fig. 4c) proposed by Nesbitt and Young (1984) can be used to identify weathering

trends of different minerals in the weathering process. In the A-CN-K diagram (Fig. 4c), the samples are generally located above the plagioclase-potassium feldspar line and have undergone certain weathering alterations. The distribution of sample points in the plagioclase gneiss fit the ideal weathering trend line well, which was close to the plagioclase to montmorillonite endpoint. The weathering process was at a stage of incongruent dissolution of plagioclase to form kaolinite (Vigil et al. 1999), which is consistent with the characterization of the SAF (Fig. 4b). The rhyolite tuff sample points were relatively scattered and were close to the potash feldspar, illite and muscovite endpoints, which are off the ideal weathering trendline. For potassium metasomatism in a volcanic matrix, clastic mixtures and diagenesis with different types of source rocks (Fedó et al. 1995; Cox et al. 1995), the increase in potassium feldspar content was related to the rock porphyry and matrix. During the weathering of volcanic rocks, the parent material and soil layer tended to be rich in K.

The CIA characterization of the degree of rock weathering does not consider the active components of Fe, Mg and P in bedrock, and volcanic rocks and plagioclase gneiss in the study area feature pyrite mineralization, including minerals such as hematite, pyrite, and apatite, with a high content of iron magnesia. The MIA index (Babechuk et al. 2014) was used to indicate the weathering dissolution characteristics of mafic minerals and to identify the redox process during the weathering process. The mineral composition of rhyolite tuff in the study area mainly consisted of light-colored minerals, with fewer dark-colored minerals. The average values of the MIA_R in soil, regolith and bedrock in the key zone were 46.81, 45.88 and 44.87, respectively, while the average MIAO values were 57.16, 55.67 and 53.79, respectively (Fig. 6). The metamorphic protolith of plagioclase gneiss was fine-grained granodiorite containing dark-colored minerals such as biotite and hornblende.

The weathering index ICV, is the ratio of the

content of relatively stable compounds in the soil to the content of compounds that are easily lost by weathering, which is suitable for determining the weathering degree. Its value increases for easily weathered rocks or minerals and decreases for relatively stable and difficult-to-weather materials. For the index value of rock and soil samples, when the $ICV > 1.0$, it indicates that the content of clay minerals in the sample is increasingly less affected by epigenetic action. An $ICV < 1.0$ indicates the opposite (Cox et al. 1995, Wu et al. 2016). The ICVs of soil, regolith and bedrock in the rhyolite tuff area ranged 0.78~1.90, 0.84~4.45, and 0.76~3.84, with average values of 1.22, 1.32, and 1.38, respectively. The coefficient of variation in the bedrock was 0.44, with a large fluctuation. The average ICV values of soil, regolith and bedrock in the plagioclase gneiss area were 1.70, 1.56, and 1.64, respectively, and these values were higher than those in the rhyolite tuff area. The average ICV values were all greater than 1.0.

3.4 REE-based mass migration coefficient tracer

Rare earth elements (REEs) are generally distributed evenly in minerals and are often used as tracer elements in petrogeochemical studies. The rare earth elements in the rock-regolith-soil system were mainly derived from bedrock and have been less affected by human input. Moreover, rare earth elements usually evolve in a coordinated manner. Rare earth elements can be used as tracer elements in

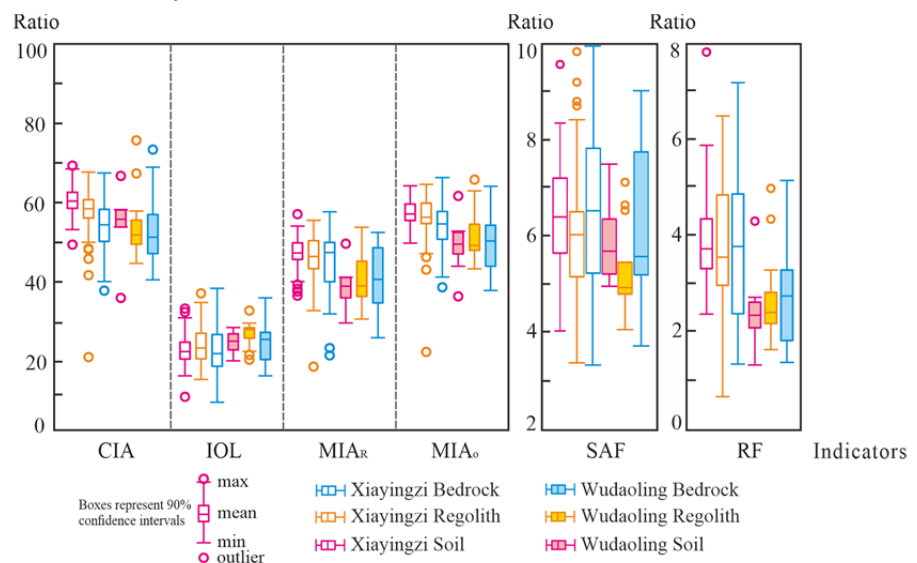


Fig. 6 Box plot of biological indexes on the bedrock-regolith-soil samples in Xiayingzi and Wudaoling geological formations.

the weathering of rock minerals into soil. In the process of rock weathering, rare earths are dissolved and released into soil solution from major minerals, fixed to secondary minerals that mainly absorb rare earth elements, and then transferred through plant absorption and organic substances (Ma et al. 2011; Fu et al. 2019).

According to the bedrock-regolith-soil layer in the rhyolite tuff formation in Xiayingzi and in the plagioclase gneiss formation in Wudaoling and the content of rare earth elements in the root of medicinal plants, a chondrite-standardized rare earth element distribution model (Fig. 7) was plotted. The average contents of light rare earth elements (LREEs), heavy rare earth elements (HREEs) and REEs in the soil, regolith and bedrock samples from the rhyolite tuff area were all higher than those from the plagioclase gneiss area. The degree of fractional LREEs and HREEs in the soil in the rhyolite tuff area was stronger than that in the plagioclase gneiss area, while the degree of fractional LREEs and HREEs in the regolith and bedrock was weaker than that in the plagioclase gneiss area. The average LREEs/HREEs ratios in the bedrock, regolith and soil in the rhyolite tuff area were 5.34, 5.24 and 4.19, while those in the plagioclase gneiss area were 8.21, 7.20 and 3.98, respectively.

The chemical depletion fraction (CDF) mainly reflects the bedrock-soil layers of elements in the weathering process of soil absolute content changes, when active strong elements after the leaching loss function cause no active elemental contents in the sample to increase. This fraction cannot truly reflect the leaching or enrichment status of elements in the process of chemical weathering, and there is a deviation in the characterization of the migration and accumulation of the active elements. To eliminate this influence, one kind of “inactive element reference system” can be used to determine the migration of the elements in the weathering rock mass relative to fresh parent rock.

The reasonableness of τ_{ij} depends on the selection of the reference elements and the determination of the reference parent rock, including Ti, Zr, Sc, Al_2O_3 , REEs, and Nb (Oeser et al. 2018; Babechuk et al. 2014). The study area is a vanadium titanomagnetite ore concentration area with a Ti element geochemical anomaly. In this study, REE inactivity was used as a reference element to calculate the bedrock-soil element mass migration coefficient

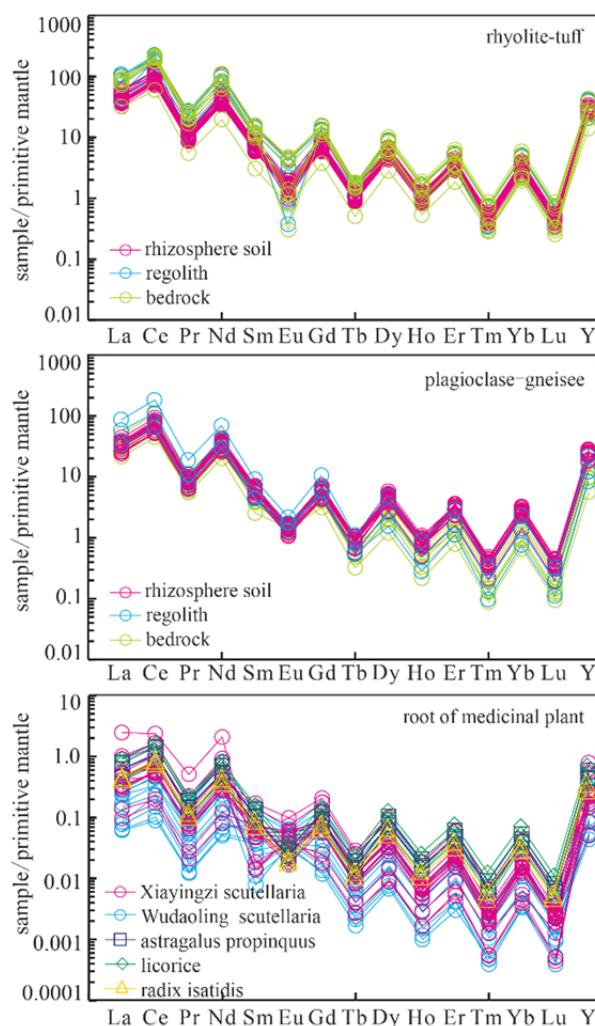


Fig. 7 Distribution of REEs in the bedrock-regolith-soil-root of the medicinal plant system.

during the weathering process. The statistical soil relative bedrock element mass migration coefficients $\tau_{soil-REE}$ in the rhyolite tuff area and in the plagioclase gneiss area are shown in Fig. 8.

The average value of the bedrock-soil element mass migration coefficient τ_{s-REE} in the rhyolite tuff formation was greater than 0, and the overall performance indicated relative REE enrichment. The enrichment intensities were ranked as $B > Cr > As > S > V > Se > Ni > Co > CaO > Cd > P > Cu > TFe_2O_3 > Mo > Pb > Ge > Mn > Zn > K_2O$. The average of τ_{s-REE} value in the plagioclase gneiss formation was significantly lower than that in the rhyolite tuff formation, with enrichment intensities ranked as $As > B > S > Cr > V > Mn > Co > Se > Mo > Ni > Cd > CaO > TFe_2O_3 > Pb > Zn > P > K_2O > Ge > o > Cu$. Except for the leaching and loss of Cu relative to rare earth elements in the plagioclase gneiss area, other

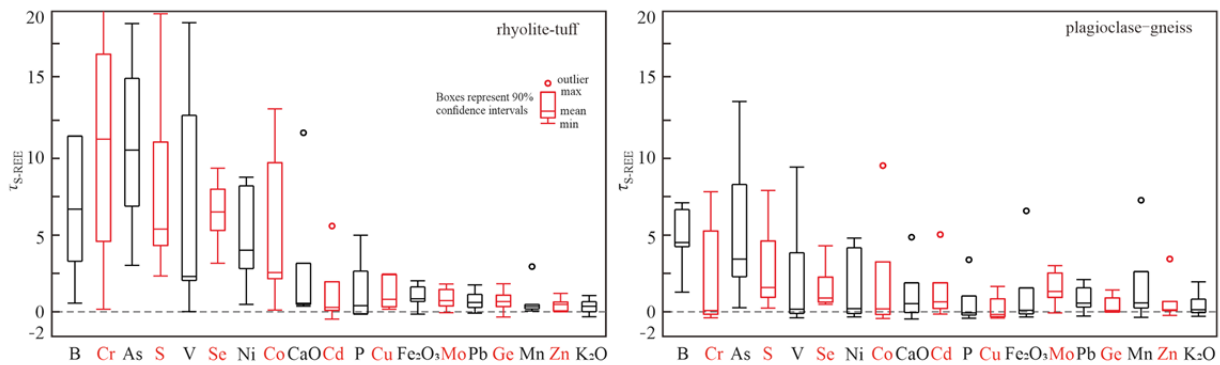


Fig. 8 Statistical box plot of the mass transfer coefficient in rhyolite-tuff and plagioclase-gneiss geological formations.

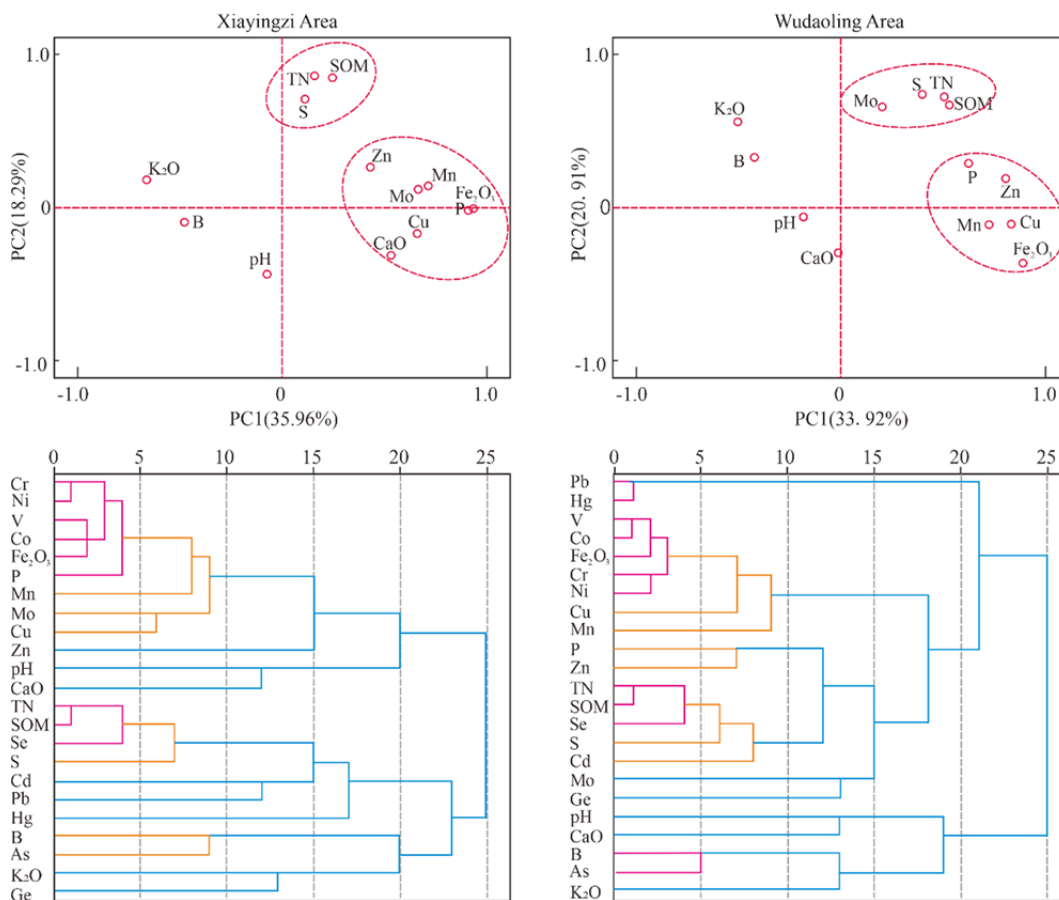


Fig. 9 Factor loading analysis and systematic clustering dendrogram of bedrock and soil samples.

elements were relatively enriched in rare earth elements during the process of rock weathering.

3.5 Correlation of surface soil elements

The factor loading analysis and systematic clustering dendrogram of the bedrock and soil samples are shown in Fig. 9. Most trace elements in the bedrock and soil are not independent minerals but often occur in the form of isomorphism in the main

mineral rock. Combined with principal component analysis and Pearson correlation system clustering analysis, this method judges the correlation changes of topsoil elements and further verifies the activity relationship between trace elements and major elements (Martignier et al. 2013).

The variances in the PC1 and PC2 eigenvalues in the principal component analysis of topsoil elemental content in the Xiayingzi area were 35.96% and 18.29%, respectively, showing high representativeness. Based

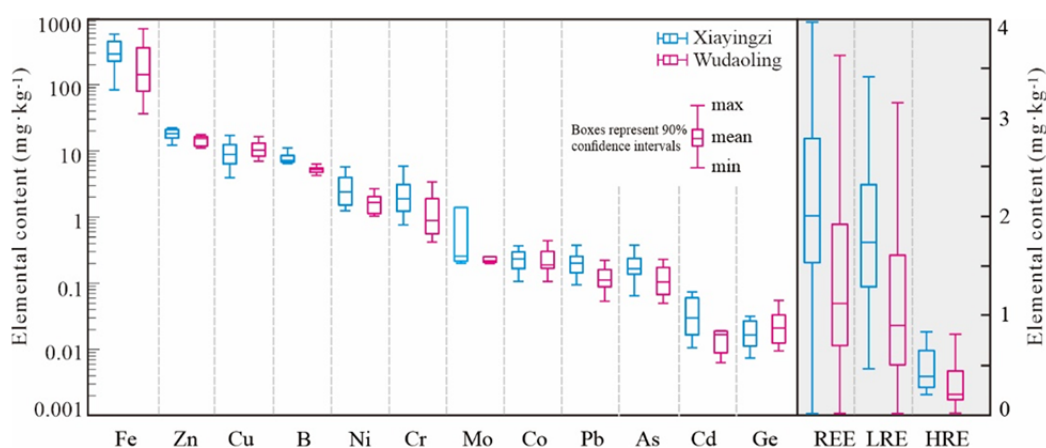


Fig. 10 Elemental contents of the samples in *Scutellaria baicalensis* Georgi in the typical study areas.

on the positive and negative load zone characteristics of elements in PC1 and PC2, Fe₂O₃, Co, Cr, Ni, P, V, Cu, Zn, Mn, Mo and CaO were grouped together; SOM, TN, Se, S, Cd and Hg were grouped together; and Pb, As, Ge and K₂O had high homology. The pH values and B elements were weakly correlated with the other variables. Pearson correlation cluster analysis showed that iron group elements, Cr, Ni, V, Co, Fe₂O₃, P, Mn, Mo, and Cu were the first group of hierarchical clusters. Elements in this group had a high correlation, and there was a certain correlation with pH and Zn and CaO contents. SOM, TN, Se, S, Cd and Hg were the second group of hierarchical clusters. The variances in the PC1 and PC2 eigenvalues in the principal component analysis of topsoil elemental content in the Wudaoling area were 33.92% and 20.91%, respectively, also with high representativeness. Based on the load matrix of the principal component analysis, the classification groups were Fe₂O₃, Co, Cr, Ni, P, V, Cu, Zn, Mn, and Ge as a group; SOM, TN, Se, S, Cd, Mo, Pb, and Hg as a group with high homology; and As, B, and K₂O as a group. The correlations of the pH value and CaO content with other variables were weak. Thus, according to the Pearson correlation clustering dendrogram, Pb and Hg were the first clustering group; iron group elements, Cr, Ni, V, Co, Fe₂O₃, Mn, and Cu were the second clustering group; and P, Zn, SOM, TN, Se, S and Cd were the third group. There were certain positive correlations between Ge and Mo, pH and CaO, and B, As and K₂O.

3.6 Overall content characteristics of the *Scutellaria baicalensis* Georgi

The elemental content of the samples in *Scutellaria baicalensis* Georgi in the study area is

shown in Fig. 10. The Fe content in the root of the *Scutellaria baicalensis* Georgi was relatively high, with a range of 84.73-849.94 mg·kg⁻¹ and an average of 347.25 mg·kg⁻¹ in Xiayingzi and with a range of 37.00~710.72 mg·kg⁻¹ and an average of 251.43 mg·kg⁻¹. The values in Wudaoling were lower than those in Xiayingzi. In Xiayingzi, the contents of Zn, Cu, Ni, Cr, and Co in the roots of the *Scutellaria baicalensis* Georgi ranged from 12.32-31.44 mg·kg⁻¹, 12.32-17.30 mg·kg⁻¹, 1.26-5.78 mg·kg⁻¹, 0.77-5.94 mg·kg⁻¹, and 0.77-5.94 mg·kg⁻¹, with averages of 18.82 mg·kg⁻¹, 9.23 mg·kg⁻¹, 2.81 mg·kg⁻¹, 2.33 mg·kg⁻¹, and 2.33 mg·kg⁻¹, respectively. The average contents of B and Mo were 8.16 mg·kg⁻¹ and 1.57 mg·kg⁻¹, respectively. The contents of Pb, Cd, and As were 0.095-0.527 mg·kg⁻¹, 0.011-0.140 mg·kg⁻¹, and 0.065-0.379 mg·kg⁻¹, respectively. The Hg content was below the detection limit. The Ge content ranged from 7.43 to 31.84 μg·kg⁻¹, with an average of 18.90 μg·kg⁻¹. The Se content was only detected at one point, 0.005 μg·kg⁻¹. The variation coefficients of Mo, Cr and LREEs in *Scutellaria baicalensis* Georgi were relatively large, and the elemental contents fluctuated greatly.

The contents of Cu, Ge and Se in the roots of *Scutellaria baicalensis* Georgi in the Wudaoling area were higher than those in the Xiayingzi area, but the contents of other elements were lower than those in the Xiayingzi area. The contents of Cu, Ge and Se ranged from 7.07-16.60 mg·kg⁻¹, 9.548-55.240 μg·kg⁻¹, and 0.009-0.111 μg·kg⁻¹, with averages of 10.71 mg·kg⁻¹, 24.007 μg·kg⁻¹, and 0.066 μg·kg⁻¹, respectively. The average contents of Zn, B, Ni, Cr, Mo and Co were 14.63, 5.26, 1.66, 1.35 and 0.22 mg·kg⁻¹, respectively. The contents of Pb, Cd, As, and Cu were 0.095-0.527, 0.011-0.140, 0.065-0.379, and 12.32-17.30 mg·kg⁻¹, respectively. The Hg content was below the detection

Table 3 Descriptive statistics of bioconcentration factors in the SPOT-*Scutellaria baicalensis* Georgi continuum in Xiayingzi and Wudaoling

| Element | Xiayingzi | | | | | Wudaoling | | | | |
|---------|-----------|-------|---------|-------|-------|-----------|-------|---------|-------|-------|
| | Min | Max | Mean | Std. | CV | Min | Max | Mean | Std. | CV |
| B | 0.145 | 0.313 | 0.188** | 0.047 | 0.250 | 0.112 | 0.160 | 0.133** | 0.014 | 0.104 |
| Cr | 0.010 | 0.105 | 0.037** | 0.025 | 0.668 | 0.007 | 0.057 | 0.022** | 0.017 | 0.756 |
| Co | 0.008 | 0.036 | 0.018 | 0.008 | 0.436 | 0.010 | 0.036 | 0.019 | 0.009 | 0.483 |
| Ni | 0.038 | 0.179 | 0.086** | 0.048 | 0.556 | 0.032 | 0.086 | 0.055* | 0.018 | 0.331 |
| Cu | 0.143 | 0.736 | 0.363 | 0.176 | 0.485 | 0.236 | 0.673 | 0.457 | 0.134 | 0.293 |
| Zn | 0.190 | 0.370 | 0.265** | 0.060 | 0.227 | 0.176 | 0.318 | 0.252** | 0.049 | 0.194 |
| As | 0.006 | 0.029 | 0.015 | 0.006 | 0.415 | 0.005 | 0.036 | 0.013 | 0.011 | 0.795 |
| Mo | 0.250 | 8.954 | 2.195* | 3.201 | 1.458 | 0.295 | 0.355 | 0.329* | 0.031 | 0.093 |
| Cd | 0.130 | 1.213 | 0.385** | 0.311 | 0.808 | 0.090 | 0.423 | 0.174* | 0.076 | 0.435 |
| Pb | 0.004 | 0.020 | 0.010** | 0.005 | 0.475 | 0.003 | 0.013 | 0.006** | 0.003 | 0.482 |
| Fe | 0.003 | 0.024 | 0.010** | 0.005 | 0.545 | 0.001 | 0.023 | 0.008** | 0.007 | 0.892 |
| Ge | 0.005 | 0.024 | 0.014 | 0.006 | 0.407 | 0.007 | 0.045 | 0.020 | 0.012 | 0.594 |
| LREE | 0.003 | 0.027 | 0.011 | 0.007 | 0.604 | 0.002 | 0.024 | 0.008 | 0.006 | 0.816 |
| HREE | 0.005 | 0.016 | 0.010 | 0.004 | 0.387 | 0.003 | 0.019 | 0.007 | 0.004 | 0.620 |
| REE | 0.003 | 0.025 | 0.011 | 0.006 | 0.550 | 0.002 | 0.023 | 0.008 | 0.006 | 0.756 |

Notes: Min represents the minimum value; Max represents the maximum value; Mean represents the average value, ** indicates the ANOVA confidence interval of the soil is less than 0.05, * indicates the ANOVA confidence interval of the soil is less than 0.1; Std. represents the standard deviation; CV represents the coefficient of variation.

limit.

The average LREE, HREE and REE contents of the *Scutellaria baicalensis* Georgi were 2173.241, 471.366 and 2644.607 $\mu\text{g}\cdot\text{kg}^{-1}$, respectively, and the average light/heavy rare earth ratio was 4.38 in Xiayingzi, while these values were 1253.298, 310.301 and 1563.600 $\mu\text{g}\cdot\text{kg}^{-1}$ and 4.07 in Wudaoling, respectively, which were significantly lower than those in Xiayingzi. The fractionation degree of light/heavy rare earth elements in the roots of the *Scutellaria baicalensis* Georgi in Wudaoling was lower than that in Xiayingzi. According to the “Green Standards of Medicinal Plants and Preparations for Foreign Trade and Economy” (WM/T2-2019), the heavy metal limits in Chinese medicinal materials are $\text{Pb} < 5.0 \text{ mg}\cdot\text{kg}^{-1}$, $\text{Cd} < 0.3 \text{ mg}\cdot\text{kg}^{-1}$, $\text{Hg} < 0.2 \text{ mg}\cdot\text{kg}^{-1}$, $\text{As} < 2.0 \text{ mg}\cdot\text{kg}^{-1}$, and $\text{Cu} < 20.0 \text{ mg}\cdot\text{kg}^{-1}$ (Zhao et al. 2010). The heavy metal contents of the samples of the *Scutellaria baicalensis* Georgi did not exceed the standard limits in the two study areas.

According to the statistical box plot of the bioconcentration coefficient (Fig. 7), the BCF values (Table 3) of trace elements in the roots of rhizosphere soil and *Scutellaria baicalensis* Georgi in Xiayingzi were ranked as $\text{Mo} > \text{Cd} > \text{Cu} > \text{Zn} > \text{B} > \text{Ni} > \text{Cr} > \text{Co} > \text{As} > \text{Ge} > \text{LREE} > \text{REE} > \text{Pb} > \text{Fe} > \text{HREE} > \text{Se}$. The bioconcentration degree of Mo was the highest, with a BCF value range of 0.250-8.954 and an average value of 2.195, which manifested as a large fluctuation range and strong uptake. The average BCF values of Cd, Cu, Zn, and B were 0.385, 0.363, 0.265, and 0.188,

respectively, which manifested as moderate uptake. The BCF values of Ni and Cr ranged from 0.038-0.179 and 0.010-0.105, with averages of 0.086 and 0.037, respectively, which manifested as weak-moderate uptake. The BCF value of Ge was 0.005-0.024, with an average of 0.014, which manifested as weak uptake. The roots of the *Scutellaria baicalensis* Georgi showed weak uptake of Co and As and extremely weak uptake of Pb, Fe, LREE, HREE and REE, with average BCF values of 0.0182, 0.0155, 0.0101, 0.0099, 0.0111, 0.0096 and 0.0108, respectively.

The BCF values of trace elements in the rhizosphere soil and *Scutellaria baicalensis* Georgi in Wudaoling were ranked as $\text{Cu} > \text{Mo} > \text{Zn} > \text{Cd} > \text{B} > \text{Ni} > \text{Cr} > \text{Ge} > \text{Co} > \text{As} > \text{Fe} > \text{LREE} > \text{REE} > \text{HREE} > \text{Pb} > \text{Se}$. Except for the bioconcentration intensity of Ge, Co, Cu, and Se in Wudaoling being higher than that in Xiayingzi, the order of BCF values of other elements was basically the same as that in Xiayingzi, whereas the enrichment intensity was lower. The average BCFs of Cu, Mo, Zn, Cd, and B elements were 0.457, 0.329, 0.252, 0.174 and 0.133, respectively, manifesting as moderate uptake. The BCF values of Ge, Ni, Cr and Co ranged 0.007-0.045, 0.032-0.086, 0.007-0.017 and 0.010-0.036, respectively, manifesting as weak uptake.

3.7 The relationship between element migration in Earth’s critical zone and the suitability of *Scutellaria baicalensis* Georgi

The contents revealed relative enrichment of

TFe₂O₃, Mn, TK, Mo, Cu, V and Co; medium levels of Ge, CaO and Zn; and relative deficiencies of TN, TP, S and SOM in the topsoil in the study area (Fig. 11). The contents of MgO, CaO, Na₂O, Hg, Cu and Cr in Wudaoling were higher than those in Xiayingzi, while the other elements showed the reverse trend. Among them, the contents of P and rare earth elements were very different, and the contents of TFe₂O₃, Al₂O₃, Co and Mo were relatively similar. There was one sample point that exceeded the standards for Cd, Cr and Ni in Xiayingzi and Hg and Zn in Wudaoling, with an exceeding rate of 0.56%. There were 3 sample points of Cu exceeding the standard, 2 sample points of Cd exceeding the standard, and 5 sample points of Cr exceeding the standard, with overstandard rates of 1.69%, 1.13% and 2.82%, respectively. The exceeding standard rate of heavy metals in soil in Wudaoling was slightly higher than that in Xiayingzi.

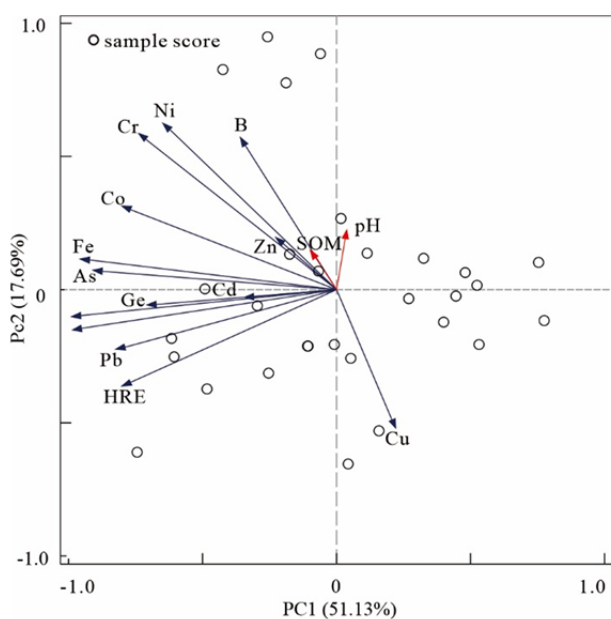


Fig. 11 Factor loading analysis of elemental content in the *Scutellaria baicalensis* Georgi.

In the weathering and pedogenetic processes of rhyolite tuff rock, B, Se, Ni, Cr, S, V, MgO, Co, Sr, Ti, TFe₂O₃ and Ge were relatively enriched, while REEs, HREEs, LREEs, Na₂O, Cu, As, Nb, Mo, Cd, K₂O, Zn, P, Mn, SiO₂, Al₂O₃, Pb and CaO were leached and lost. In plagioclase gneiss, B, As, Se, S, LREEs, Mo, Ge, REEs, Cd, Ti, Pb and HREEs were relatively enriched, and Cu, Sr, Na₂O, MgO, P, Co, CaO, K₂O, Cr, TFe₂O₃, Zn, V, Al₂O₃, SiO₂, Mn and Ni were leached and lost. The leaching loss of CaO, Al₂O₃ and Cu in the rhyolitic tuff formation was stronger than that in the plagioclase

gneiss formation, but the leaching loss of P, SiO₂, Na₂O, K₂O, Zn and Mn was weaker. In the process of weathering and pedogenesis, TFe₂O₃, Ni, V, Cr, Co, MgO and Sr were shown to have relative enrichments in the rhyolitic tuff formation, whereas these were shown as leaching losses in the plagioclase gneiss formation. Rare earth elements (REEs, LREEs and HREEs), Cd, Nb, Mo, Pb and As were relatively enriched in soil in the plagioclase gneiss formation, whereas leaching loss occurred in the rhyolitic tuff formation. This was related to the interaction of elemental abundance in the parent rock and human influence.

4 Conclusions

This article selected plagioclase gneiss and rhyolite tuff study areas and utilized the elemental contents, chemical weathering index, elemental chemical loss fraction, mass transfer coefficient method, and biological enrichment coefficient to study BRSP system elemental migration and accumulation, heavy metals, and rare earth elements that have consistently moved in a key mountainous area on Earth. Results showed that the studied soils have the characteristics of product materials. Through BRSP system research, this paper determined the system's overall dynamic characteristic elements and behaviours for appropriate genetic background characteristic identification in medicinal materials directional cultivation planning and site selection and provided data support. Furthermore, from the perspective of Earth system science, this paper studied rock weathering crust-soil-medicinal plant element migration and accumulation and terrestrial ecological and geochemical characteristics, thus broadening the content of past research to focus more on the effective components of the *Scutellaria baicalensis* Georgi and the causes of the fingerprint, pharmacology, environmental conditions, etc., of different medicinal plants on soil parent material, broadening the scope of Earth system science research that has been explored.

Acknowledgments

The authors would like to thank the editor and anonymous reviewers for their valuable comments

that greatly improved this work. This research was funded by the China Geological Survey, grant number DD20190822.

References

- Alaimo MG, Dongarra G, La RA, et al. (2018) Major and trace elements in *Boletus aereus* and *Clitopilus prunulus* growing on volcanic and sedimentary soils of Sicily (Italy). *Ecotoxicol Environ Saf* 157: 182-190.
<https://doi.org/10.1016/j.ecoenv.2018.03.080>
- Amber AB, Viqar S (2015) Inhibition of transforming growth factor - β (TGF- β) signaling by *Scutellaria baicalensis* and *Fritillaria cirrhosa* extracts in endometrial cancer. *J Cell Biochem* 116(8): 1797-1805.
<https://doi.org/10.1002/jcb.25138>
- Anderson RS (2015) Pinched topography initiates the critical zone. *Science* (N.Y.) 350(6260): 506-512.
<https://doi.org/10.1126/science.aad2266>
- An PJ, Zhang ZQ, Wang LW (2016) Review of Earth critical zone research. *Adv Earth Sci* 31(12): 1228-1234.
<https://doi.org/10.11867/j.issn.1001-8166.2016.12.1228>
- An YL, Huang Y, Sun Z, et al. (2018) Chemical speciation and bioavailability of five heavy metals in soil of Beijing plain area in two years. *Geol Bull China* 37(6): 1142-1149.
<https://doi.org/10.3969/j.issn.1671-2552.2018.06.016>
- Babechuk MG, Widdowson M, Kamber BS (2014) Quantifying chemical weathering intensity and trace element release from two contrasting basalt profiles, Deccan Traps, India. *Chem Geol* 363: 56-75.
<https://doi.org/10.1016/j.chemgeo.2013.10.027>
- Basic research opportunities in the Earth Sciences board on earth sciences and resources (2000) Basic research opportunities in Earth Sciences. Washington DC: National academies press, 35-45.
<https://doi.org/10.17226/9981>
- Brantley SL, Goldhaber MB, Ragnarsdottir KV (2007) Crossing disciplines and scales to understand the critical zone. *Elements* 3(5):307-314.
<https://doi.org/10.2113/gselements.3.5.307>
- Braude MR, Bassily R (2019) Drug-induced liver injury secondary to *Scutellaria baicalensis* (Chinese skullcap). Primary sources for research and education 49(4): 544-546.
<https://doi.org/10.1111/imj.14252>
- Chadwick OA, Brimhall GH, Hendricks DM (1990) From a black box to a gray box: A mass balance interpretation of pedogenesis. *Geomorphology* 3: 369-390.
[https://doi.org/10.1016/0169-555X\(90\)90012-F](https://doi.org/10.1016/0169-555X(90)90012-F)
- Cheng CS, Chen J, Tan HY et al. (2018) *Scutellaria baicalensis* and cancer treatment: recent progress and perspectives in biomedical and clinical studies. *Am J Chin Med* 46(1): 25-54. (In Chinese)
- Cox R, Lowe DR, Cullers RL (1995) The influence of sediment recycling and basement composition on evolution of mudrock chemistry in the southwestern United States. *Geochim Cosmochim Acta* 59(14): 2919-2940.
[https://doi.org/10.1016/0016-7037\(95\)00185-9](https://doi.org/10.1016/0016-7037(95)00185-9)
- Eduardo G, Marta P, Massimo S et al. (2014) Provenance versus weathering control on the composition of tropical river mud (southern Africa). *Chem Geol* 366: 61-74.
<https://doi.org/10.1142/S0192415X18500027>
- Fedo CM, Nesbitt HW, Young GM (1995) Unraveling the effects of potassium metasomatism in sedimentary rocks and paleosols, with implications for paleoweathering conditions and provenance. *Geology* 23(10): 921-924.
[https://doi.org/10.1130/0091-7613\(1995\)0232.3.CO;2](https://doi.org/10.1130/0091-7613(1995)0232.3.CO;2)
- Fu W, Luo P, Hu ZY et al. (2019) Enrichment of ion-exchangeable rare earth elements by felsic volcanic rock weathering in South China: genetic mechanism, formation preference. *Ore Geol Rev* 114(9): 103-120.
<https://doi.org/10.1016/j.oregeorev.2019.103120>
- Guo LP, Wang S, Zhang J et al. (2013) Effects of ecological factors on secondary metabolites and inorganic elements of *Scutellaria baicalensis* and analysis of geoherblism. *Sci China Life Sci* 56(11): 1047-1056.
<https://doi.org/10.1007/s11427-013-4562-5>
- Guo M, Wu ZL, Wang CG et al. (2014) Synthesis and anti-tumor activity of baicalin-metal complex. *Acta Pharm Sin* 49(3): 337-345.
<https://doi.org/10.16438/j.0513-4870.2014.03.004>
- He HL, Yu SY, Song XY et al. (2016) Origin of nelsonite and Fe-Ti oxides ore of the Damiao anorthosite complex, NE China: Evidence from trace element geochemistry of apatite, plagioclase, magnetite and ilmenite. *Ore Geol Rev* 79: 367-381.
<https://doi.org/10.1016/j.oregeorev.2016.05.028>
- Hewawasam T, Blanckenburg FV, Bouchez J et al. (2013) Slow advance of the weathering front during deep, supply-limited saprolite formation in the tropical Highlands of Sri Lanka. *Geochim Cosmochim Acta* 118: 202-230.
<https://doi.org/10.1016/j.gca.2013.05.006>
- Holl R, Kling M, Schroll E (2007) Metallogenesis of Germanium-A review. *Ore Geol Rev* 30: 145-180.
<https://doi.org/10.1016/j.oregeorev.2005.07.034>
- Jin BR, Chung KS, Kim HJ et al. (2019) Chinese skullcap (*Scutellaria baicalensis* Georgi) inhibits inflammation and proliferation on benign prostatic hyperplasia in rats. *J Ethnopharmacol* 235: 481-488.
<https://doi.org/10.1016/j.jep.2019.01.039>
- Kong WW (2008) Evaluation of quality and ecological suitability of *Scutellaria*. Jilin: Jilin Agricultural University.
<https://doi.org/10.7666/d.y1511981>
- Laila M, Naaila O, Abdessamed H, et al. (2019) Accumulation of heavy metals in metallophytes from three mining sites (Southern Centre Morocco) and evaluation of their phytoremediation potential. *Ecotoxicol Environ Saf* 169: 150-160.
<https://doi.org/10.1016/j.ecoenv.2018.11.009>
- Lam W, Bussom S, Guan FL et al. (2010) The four-herb Chinese medicine PHY906 reduces chemotherapy-induced Gastrointestinal toxicity. *Sci Transl Med* 2(45): 45-59.
<https://doi.org/10.1126/scitranslmed.3001270>
- Li LX, Li HM, Zi JW et al. (2019) Role of fluids in Fe-Ti-P mineralization of the Proterozoic Damiao anorthosite complex, China: Insights from baddeleyite-zircon relationships in ore and altered anorthosite. *Ore Geol Rev* 115:103186.
<https://doi.org/10.1016/j.oregeorev.2019.103186>
- Lin H (2010) Earth's critical zone and hydrogeology: concepts, characteristics, and advances. *Hydrol Earth Syst Sci* 14: 25-45.
<https://doi.org/10.5194/hess-14-25-2010>
- Luo Y, Lv YH, Fu BJ, et al. (2019) When multi-functional landscape meets critical zone science: advancing multi-disciplinary research for sustainable human well-being. *Natl Sci Rev* 6(2): 349-358.
<https://doi.org/CNKI:SUN:NASR.o.2019-02-033>
- Lv YH, Li T, Zhang K, et al. (2017) Fledging critical zone science

- for environmental sustainability. *Environ Sci Technol* 51(15): 8209-8211.
<https://doi.org/10.1021/acs.est.7b02677>
- Ma L, Jin LX, Brantley LS (2011) How mineralogy and slope aspect affect REE release and fractionation during shale weathering in the Susquehanna/Shale Hills critical zone Observatory. *Chem Geol* 290(1-2): 31-49.
<https://doi.org/10.1016/j.chemgeo.2011.08.013>
- Martignier L, Verrecchia PE (2013) Weathering processes in superficial deposits (regolith) and their influence on pedogenesis: A case study in the Swiss Jura Mountains. *Geomorphology* 189:26-40.
<https://doi.org/10.1016/j.geomorph.2012.12.038>
- Ministry of Land and Resources, PRC (2016) Analysis methods for regional geochemical sample. DZ/T 0279-2016. Beijing. Geological Publishing House. Available online at: http://g.mnr.gov.cn/201701/t20170123_1430106.html (Accessed on 16 August 2016)
- Moses C, Robinson D, Barlow J (2014) Methods for measuring rock surface weathering and erosion: A critical review. *Earth Sci Rev* 135:141-161.
<https://doi.org/10.1016/j.earscirev.2014.04.006>
- Nesbitt HW, Young GM (1982) Early Proterozoic climates and plate motions inferred from major element chemistry of lutites. *Nature* 299:715-717.
<https://doi.org/10.1038/299715a0>
- Nesbitt HW, Young GM (1984) Prediction of some weathering trends of plutonic and volcanic rocks based on thermodynamic and kinetic considerations. *Geochim Cosmochim Acta* 48(7): 1523-1534.
[https://doi.org/10.1016/0016-7037\(84\)90408-3](https://doi.org/10.1016/0016-7037(84)90408-3)
- Oeser RA, Stroncik N, Moskwa LM et al. (2018) Chemistry and microbiology of the critical zone along a steep climate and vegetation gradient in the Chilean Coastal Cordillera. *Catena* 170:183-203.
<https://doi.org/10.1016/j.catena.2018.06.002>
- Pan LL (2011) Study on the medicinal materials quality of *Scutellaria baicalensis* Georgi and its ecological attitudes. Jilin: Jilin Agricultural University. (In Chinese)
- Peng B, Rate A, Song ZL et al. (2014) Geochemistry of major and trace elements and Pb-Sr isotopes of a weathering profile developed on the Lower Cambrian black shales in central Hunan, China. *Appl Geochemistry* 51:191-203.
<https://doi.org/10.1016/j.apgeochem.2014.09.007>
- Qiu SF, Zhu ZY, Yang T et al. (2014) Chemical weathering of monsoonal eastern China: implications from major elements of topsoil. *J Asian Earth Sci* 81(4):77-90.
<https://doi.org/10.1016/j.jseas.2013.12.004>
- Richter DD, Billings SA (2015) One physical system: Tansley's ecosystem as Earth's critical zone, Tansley review. *New Phytol* 206(3): 900-912.
<https://doi.org/10.1111/nph.13338>
- Sun HY, Sun XM, Jia FC et al. (2020) The eco-geochemical characteristics of germanium and its relationship with the genuine medicinal material *Scutellaria baicalensis* in Chengde, Hebei Province. *Geol China* 47(6):1646-1667.
<https://doi.org/10.12029/gc20200604>
- Vigil R, Cala V, García RJ et al. (1993) Clay genesis in textural contrasted soils in semiarid conditions. *Min. Petrogr. Acta*. XXXV 253-259.
- Vigil R, García R, Rubio RJ et al. (1999) Soil Alteration processes on granite in the central mountain range (Spain). *Zeitschrift für Geomorphologie*, NF 44-2: 233-248.
- Wang S, Zhao MX, Guo LP et al. (2014) The content of inorganic elements of *Scutellaria baicalensis* from different origins and its relationship with inorganic elements in relevant rhizosphere soil. *Acta Ecol Sin* 34(16): 4734-4745.
<https://doi.org/10.5846/stxb201304160722>
- Wang ZL, Deng TD, Wang RM et al. (2009) Characteristics of migration and accumulation of rare earth elements in the rock-soil-navel orange system. *Geol China* 36(6): 1382-1394. (In Chinese)
- Wang ZL, Wang S, Yi K, et al. (2018) A comprehensive review on phytochemistry, pharmacology, and flavonoid biosynthesis of *Scutellaria baicalensis*. *Pharm Biol* 56(1): 465-484.
<https://doi.org/10.1080/13880209.2018.1492620>
- Wen XF, Zhang XY, Wei J, et al. (2019) Understanding the Biogeochemical Process and Mechanism of Ecosystem Carbon Cycle from the Perspective of the Earth's critical zone. *Adv Earth Sci* 34(5): 471-479.
<https://doi.org/10.11867/j.issn.1001-8166.2019.05.0471>
- Wu BJ, Peng B, Zhang K, et al. (2016) A new chemical index of identifying the weathering degree of black shales. *Acta Geol Sin* 90(4): 818-832. (In Chinese)
- Wu NX, Meng SX, Ren Y, et al. (2016) Elemental migration characteristics and chemical weathering degree of black shale in Northeast Chongqing, China. *Earth Sci* 41(2): 218-233.
<https://doi.org/10.3799/dqkx.2016.017>
- Xu N, Meng FY, Zhou GF, et al. (2020) Assessing the suitable cultivation areas for *Scutellaria baicalensis* in China using the Maxent model and multiple linear regression. *Biochem Syst Ecol* 90:104052
<https://doi.org/10.1016/j.bse.2020.104052>
- Yang Y, Zhou XH, Tie BQ, et al. (2017) Comparison of three types of oil crop rotation systems for effective use and remediation of heavy metal contaminated agricultural soil. *Chemosphere* 188: 148-156.
<https://doi.org/10.1016/j.chemosphere.2017.08.140>
- Zhang GL, Zhu YG, Shao MG (2019) Understanding sustainability of soil and water resources in a critical zone perspective. *Science China Earth Sci* 62: 1716-1718.
<https://doi.org/10.1007/s11430-019-9368-7>
- Zhang M, Chen SL, Seto S et al. (2009) Correlation of antioxidative properties and vaso-relaxation effects of major active constituents of traditional Chinese medicines. *Pharm Biol* 47(4): 366-371.
<https://doi.org/10.1080/13880200902753064>
- Zhang ZC, Santosh M, Li JW (2015) Iron deposits in relation to magmatism in China. *J Asian Earth Sci* 113(3): 951-956.
<https://doi.org/10.1016/j.jseas.2015.09.026>
- Zhao MX, Lv JR, Guo LP, et al. (2010) Effects of inorganic elements of soil on contents of inorganic elements and baicalin in *Scutellaria*. *Chinese J Exp Tradit Med Formul* 16(9): 103-106.
<https://doi.org/10.13422/j.cnki.syfjx.2010.09.068>
- Zhao Q, Chen XY, Martin C (2016a) *Scutellaria baicalensis*, the golden herb from the garden of Chinese medicinal plants. *Sci Bull* 61(18): 1391-1398.
<https://doi.org/10.1007/s11434-016-1136-5>
- Zhao Q, Zhang Y, Wang G, et al. (2016b) A specialized flavone biosynthetic pathway has evolved in the medicinal plant, *Scutellaria baicalensis*. *Sci Adv* 2(4): 1-15.
<https://doi.org/10.1126/sciadv.1501780>
- Zhao Q, Cui MY, Levsh O et al. (2018) Two CYP82D Enzymes function as flavone hydroxylases in the biosynthesis of root-specific 4'-Deoxyflavones in *Scutellaria baicalensis*. *Mol Plant* 11(1): 135-148.
<https://doi.org/10.1016/j.molp.2017.08.009>
- Zhi HJ, Jin X, Zhu HY et al. (2020) Exploring the effective materials of flavonoids-enriched extract from *Scutellaria baicalensis* roots based on the metabolic activation in influenza a virus induced acute lung injury. *J Pharm Biomed Anal* 177: 112876.
<https://doi.org/10.1016/j.jpba.2019.112876>
- Zhu YG, Duan GL, Chen BD et al. (2014) Mineral weathering and element cycling in soil-microorganism-plant system. *Sci China: Earth Sci* 57(5): 888-896.
<https://doi.org/10.1007/s11430-014-4861-0>
- Zhu YG, Li G, Zhang GL et al. (2015) Soil security: From Earth's critical zone to ecosystem services. *Acta Geogr Sin* 70(12): 1859-1869.
<https://doi.org/10.11821/dlxb201512001>